Sedimentologic evidence for a major paleogeographic change at 8.5–6.5 Ma near San Antonio, south-central New Mexico

Daniel J. Koning, Kevin M. Hobbs, Andrew P. Jochems, and Richard M. Chamberlin
2022, pp. 221-238. https://doi.org/10.56577/FFC-72.221
Supplemental data: https://nmgs.nmt.edu/repository/index.cfml?rid=2022002

in:

Socorro Region III, Koning, Daniel J.; Hobbs, Kevin J.; Phillips, Fred M.; Nelson, W. John; Cather, Steven M.; Jakle, Anne C.; Van Der Werff, Brittney, New Mexico Geological Society 72nd Annual Fall Field Conference Guidebook, 426 p. https://doi.org/10.56577/FFC-72

This page is intentionally left blank to maintain order of facing pages.

New Mexico Geological Society Guidebook, 72nd Fall Field Conference, 2022, p. 221–238.

SEDIMENTOLOGIC EVIDENCE FOR A MAJOR PALEOGEOGRAPHIC CHANGE AT 8.5–6.5 MA NEAR SAN ANTONIO, SOUTH-CENTRAL NEW MEXICO

DANIEL J. KONING[1], KEVIN M. HOBBS[1], ANDREW P. JOCHEMS[1], AND RICHARD M. CHAMBERLIN[1]

[1]New Mexico Bureau of Geology and Mineral Resources, New Mexico Institute of Mining and Technology, 801 Leroy Place, Socorro, NM 87801; dan.koning@nmt.edu

Abstract—West of San Antonio, in southern Socorro County, the 8.5 Ma basalt of Broken Tank is used to document a broad, westward-sloping piedmont that extended across preexisting, east-tilted fault blocks that now comprise the core of the Chupadera Mountains. Prior to 8.5 Ma, fingers of the west-sloping piedmont filled shallow paleovalleys cut across hilly paleotopography of the early Chupadera Mountains. The coarse piedmont sediment is part of the Popotosa Formation, which extends ~460 m below and ~180 m above the basalt of Broken Tank. In Nogal Canyon, 7 km west of San Antonio, we measured a stratigraphic section and collected paleoflow, clast composition, and clast size data in the Popotosa Formation within 35 m below and 65 m above the 40 m thick basalt. These data indicate a change in piedmont provenance and paleoflow after the emplacement of the basalt. Crystal-poor rhyolite clasts are slightly more abundant (about 10%) below the basalt and are similar to upper Luis Lopez "moat rhyolite" lava locally exposed below the Popotosa Formation. Paleoflow was clearly southwest-directed in strata below the basalt. Immediately above the basalt lies a 1.5 m bed of silty very fine– to fine-grained sandstone (possibly eolian), which is overlain by 8 m of a coarsening-upward pebbly sandstone to pebbly conglomerate. The 55 m of overlying strata coarsen upwards from a pebble conglomerate–pebbly sandstone, interbedded with two fine-grained beds interpreted as basin-floor facies, to a boulder-bearing conglomerate. This coarsening-upward trend, combined with northeast to southeast paleoflow indications, is consistent with eastward piedmont progradation. These data and observations indicate a major paleogeographic change after the basalt of Broken Tank was emplaced at 8.5 Ma. Prior to the basalt, volcanic gravel and sand derived from the Quebradas region, with an inferred additional contribution from a postulated paleotopographic high near the modern-day village of Luis Lopez, was deposited on a southwest-sloping piedmont. After the basalt emplacement, sometime between 8.5–6.5 Ma, the southwest-flowing piedmont was replaced by a southeast-sloping piedmont sourced in the eastern Magdalena Mountains, consistent with the provenance of a unique clast type in the upper Lemitar Tuff. The cause of this "piedmont reversal" is ascribed to increased slip rates on faults east of the Rio Grande, which caused collapse and burial of the southwest-sloping piedmont and the inferred Luis Lopez paleotopographic high; this reversal also resulted in an eastward shift in basin floor facies toward the modern Rio Grande. This tectonically driven paleogeographic change would have lowered the southern sill of the late Miocene playa presumed to be the terminus of the ancestral Rio Grande, facilitating the southward integration of the Rio Grande in the latest Miocene–earliest Pliocene.

INTRODUCTION

Detailed sedimentologic study of Miocene-age stratigraphic intervals in the Santa Fe Group, the clastic sediment filling the Rio Grande rift, yields clues regarding paleo-drainage evolution. For example, in the northeastern Española Basin, close inspection of clastic (sand and gravel) material and paleoflow indicators supports interpretation of two paleo-drainages that shifted laterally in the middle Miocene, ultimately with one prograding over the other (Cavazza, 1986; Manley, 1976, 1979; Koning, 2002, 2003; Koning and Manley, 2003; Koning et al., 2005, 2013). Sedimentologic studies of shifting paleo-drainages and/or source-area changes in the Rio Grande rift include the Culebra graben of the San Luis Basin (Armstrong et al., 2013), west-central Española Basin (Ingersoll et al., 1990; Smith, 2004), northwest Albuquerque Basin (Connell et al., 1999; Koning and Personius, 2002; Koning et al., 2020), southwest Albuquerque Basin (Lozinsky and Tedford, 1991), northern boundary of the Socorro-La Jencia basins (Cather and Read, 2003; Chamberlin, 1999), and the Rincon area 140 km to the south (Mack et al., 1994; Seager and Mack, 2003).

In the Rio Grande rift, tectonic activity and paleoclimatic changes have been invoked as the main drivers for paleo-drainage evolution. The axial river, the ancestral Rio Grande, has captured the most attention in this regard because of its size and robust documentation of its downstream integration across previously closed basins at the beginning of the Pliocene (Hawley et al., 1969; Gustavson, 1991; Mack et al., 1993, 1998, 2006; Seager and Mack, 2003; Mack, 2004; Connell et al., 2005; Repasch et al., 2017; Koning et al., 2016a, 2018). Hypotheses for integration drivers include tectonic uplift in the Rio Grande headwaters (Kottlowski, 1953; Repasch et al., 2017), decrease in rift extension rates and accompanying decreasing basin subsidence rates (Connell et al., 2005; Koning et al., 2016a), and increased water discharges (Chapin, 2008; Koning et al., 2016a, 2016b). Changes in the size of large, oblique tributary fans (e.g., ancestral Rio Puerco) and piedmont drainage systems have been ascribed to paleoclimate changes (Connell et al., 2013) or changes in fault activity that influenced locations (loci) of maximum subsidence within a rift basin (e.g., Española Basin; Smith, 2004; Koning et al., 2013). In one classic study, the exhumation of the Caballo Mountains has been documented by changes in gravel composition (Mack et al., 1994). Exhumation there was accompanied by high extensional strain rates in the latest Miocene that reorganized fault networks and created more, but narrower, basins compared to the earlier, broader rift basins in the area (Mack et al., 1994; Seager and Mack, 2003).

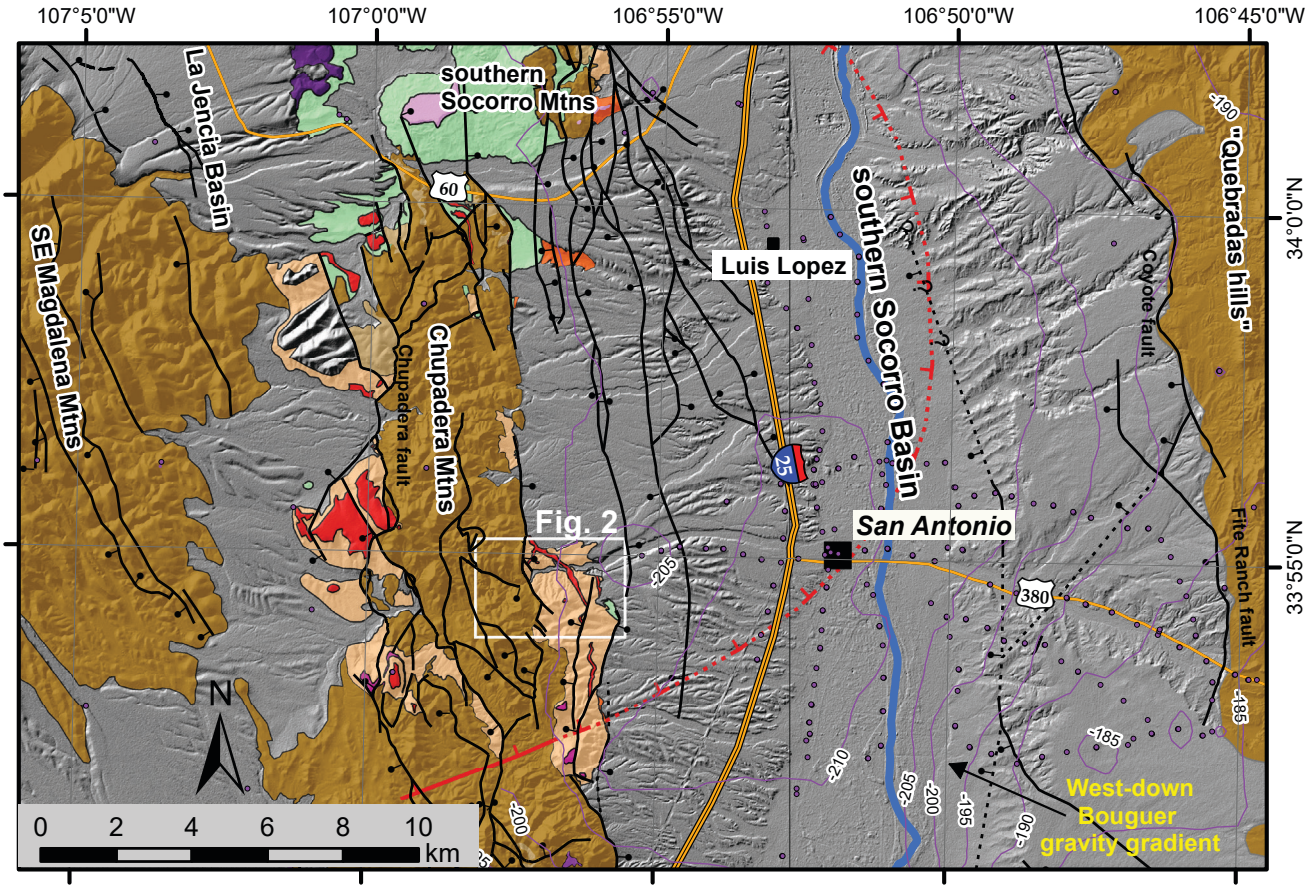

Upper Santa Fe Group and post-Santa Fe Group (Plio-Pleistocene)

Clear — Sierra Ladrones Formation and younger alluvium (Plio-Pleistocene) -- Weakly consolidated gravel and sand.

Basalt of Socorro Canyon

Lower to Middle Santa Fe Group (Miocene)

Popotosa-Sierra Ladrones transitional facies (Upper Miocene) -- Interbedded sand, mud, and pebbly sand.

Popotosa Formation, upper conglomeratic strata (Upper Miocene) -- Sandstone and conglomerate; not strongly cemented by jasperoids.

Popotosa Formation, playa deposits (8.5-11 Ma) -- Reddish brown clay; sand tongues to north.

Late Miocene mafic flows

Basaltic andesite of Sedillo Hill (7.0 Ma)

Basalt of Broken Tank (8.5 Ma)

Basalt of Chupadera Spring (9.8 Ma)

Bedrock, undivided

Well-cemented volcanic rocks, lower Santa Fe Group, Baca Formation, Cretaceous, Pennsylvanian, and Permian strata; also Proterozoic crystalline rocks

Normal fault -- dashed where approximately located, dotted where concealed.

Gravity Station (from PACES, 2021)

complete Bouguer gravity anomaly contour (mGals); assumed bedrock density of 2.67 g/cm^3

Socorro caldera margin (from Chamberlin, 2004); hatched lines show inside of caldera, corresponding with thick Luis Lopez Fm; dotted where buried

FIGURE 1. Map showing geographic context and simplified geology of the Chupadera Mountains and southern Socorro Basin. The Rio Grande (heavy blue line) flows south through the southern Socorro Basin. Gravity point data obtained from PACES (2021) and associated contours show the complete Bouguer gravity anomaly (courtesy of Marissa Fischera). Concealed (dotted) faults on the east side of the Rio Grande floodplain and west of the Quebradas, north of Highway 380, are inferred using these gravity data and previously mapped faults (from the USGS Quaternary faults and folds database; USGS, 2022). Bedrock geology of the Quebradas hills simplified from NMBGMR (2003). Bedrock geology for the Chupadera and Socorro Mountains is simplified from Chamberlin et al. (2002) and Chamberlin (1999). Outline of Socorro caldera, which can be assumed to host at least several hundred meters of Luis Lopez Formation, is from Chamberlin et al. (2004).

Motivation for Study

The 8.5 Ma basalt of Broken Tank acts as a stratigraphic time marker for which to interpret the paleogeography of the Socorro Basin. This feature is found 10–23 km southwest of Socorro on either side of the Chupadera Mountains and as small remnants in the middle of these mountains (Fig. 1). Depositional facies and stratigraphic relations from outcrops underlying this basalt indicate that it flowed down a west-sloping piedmont on the east side of the mountains and then continued westward through paleovalley(s) incised into bedrock near the modern-day crest of the mountains (Chamberlin et al., 2002). In other words, a major paleogeographic high was present east of the Chupadera Mountains that produced sufficient sediment to form a west-sloping piedmont extending across the Chupadera Mountains, which were poking upward through the piedmont paleo-surface as scattered hills. On the west side of the mountains, the basalt flowed west and northwest down alluvial fans before extending onto a playa floor located north of these fans (Chamberlin et al., 2002). The basalt of Broken Tank has been dated in 10 areas across the Chupadera Mountains, yielding a mean $^{40}Ar/^{39}Ar$ age of 8.54±0.20 Ma (see Day 2 road log; Koning et al., this volume).

Preliminary inspection by the lead author of well-exposed outcrops 7 km west of San Antonio in Nogal Canyon (also known as Walnut Canyon) suggested a change in gravel composition above the basalt compared to below it. Furthermore, preliminary observation of paleocurrent indicators suggested that a change in paleoflow accompanied this change in gravel composition (S. Cather, pers. commun., 2015). Given the location of these outcrops southeast of a large playa representing the terminus of the Rio Grande in the early late Miocene (D. Koning, unpublished data), understanding how the paleotopography and paleogeography changed in the latest Miocene could lead to better understanding of how the ancestral Rio Grande integrated through what was once a closed basin. Thus, we gathered a robust set of sedimentologic data at the study area to test whether paleo-drainage systems did indeed change after emplacement of basalt of Broken Tank and to interpret the implications of this change for paleogeography, tectonics, and ancestral Rio Grande integration.

Geologic Setting

The study site is located in Nogal Canyon, 7 km west of San Antonio at the eastern margin of the Chupadera Mountains (Fig. 1). The Chupadera Mountains are cored mainly by early Oligocene volcanic rocks, with Popotosa Formation outcrops (lower-middle Santa Fe Group) concentrated on their northern ends and locally along their foothills (Fig. 1). Volcanic rocks filled two overlapping calderas in the early Oligocene: the 32.35±0.01 Ma Socorro caldera and the 29.00±0.01 Ma Sawmill caldera (ages from Chamberlin et al., 2004, adjusted for a FCT sanidine monitor age of 28.201 Ma). These volcanic rocks are composed mainly of rhyolitic ignimbrites, felsic to mafic flows, ash-fall tuffs, and volcaniclastic sediment. An important formation for our study is the Luis Lopez Formation, which consists of a 1100 m thick succession of intermediate to rhyolite-basalt flows, phenocryst-poor tuffs, and volcaniclastic sediment that filled the Socorro caldera between 32.3 Ma and 29.0 Ma (Chamberlin et al., 2004; see Fig. 1 for outline of caldera and corresponding extent of Luis Lopez Formation). The top of the Luis Lopez Formation near our study area consists of crystal-poor rhyolite domes (Chamberlin et al., 2002; Chamberlin et al., 2004).

Figure 2 shows the location of $^{40}Ar/^{39}Ar$ samples of the basalt of Broken Tank interbedded in the Popotosa Formation near the study site. The closest sample had an age of 10.23±0.60 Ma (FCT monitor age of 28.201 Ma) that is considered unreliable because it came from an altered corestone. We prefer the age collected from the same flow 1.8–1.9 km to the south (NM 1531), which yielded a published age of 8.36±0.05 Ma (Chamberlin et al., 2002, Table 1, FCT sanidine monitor age of 27.84 Ma); correcting for the updated FCT monitor age of 28.201 Ma results in an age of 8.47±0.05 Ma.

The east-tilted Chupadera Mountains are part of a structural high that continues northward to include the west-tilted Socorro and Lemitar Mountains. This structural high can be considered as an inter-graben uplift within the Rio Grande rift, separating the La Jencia Basin on the west from the Socorro Basin on the east. Bedrock strata in the Chupadera Mountains tilt 20–30° to the east, the tilting facilitated by west-down motion along the Chupadera fault bounding the western foot of the mountains (Fig. 1). The eastward dip of the Chupadera Mountains likely continues in bedrock strata and Popotosa Formation (Santa Fe Group) strata under the eastern part of the adjoining Socorro Basin (Chamberlin et al., 2002). Several faults offset Quaternary sediment in the piedmont between the Chupadera Mountains and the Rio Grande, mostly exhibiting an east-down sense of throw. More detail of the bedrock geology of the Chupadera Mountains can be found in Eggleston (1982), Eggleston et al. (1983), Chamberlin et al. (2002, 2004), and Chamberlin and Cikoski (2010).

On the north side of the Chupadera Mountains are well-cemented conglomerates and sandstones of the lower to middle Popotosa Formation, overlain by hundreds of meters of clays deposited by a playa lake system in the early part of the late Miocene (Chamberlin, 1999; Chamberlin et al., 2002). Sand tongues interbedded in the playa clays increase in abundance to the north. Ongoing work on these sand tongues suggest a sand composition similar to Plio-Pleistocene, ancestral Rio Grande sand, but this needs to be confirmed by additional petrography and detrital sanidine analyses; moreover, sedimentary structures and lithostratigraphic assemblages are consistent with deltaic-fluvial facies (D. Koning, unpublished data). Nowhere in the northwestern Chupadera Mountains has playa sediment been observed beneath the ~11 Ma rhyolite of Pound Ranch, and playa deposits are not preserved on top of the 6.97±0.02 Ma basaltic andesite of Sedillo Hill (Chamberlin and Osburn, 2006). Therefore, it is interpreted that these clays and sand tongues are associated with the terminal playa of the Rio Grande, and the age of this playa spanned 11 to 6.5–7 Ma in the northern Chupadera Mountains area.

The Socorro Basin can be subdivided into a northern and

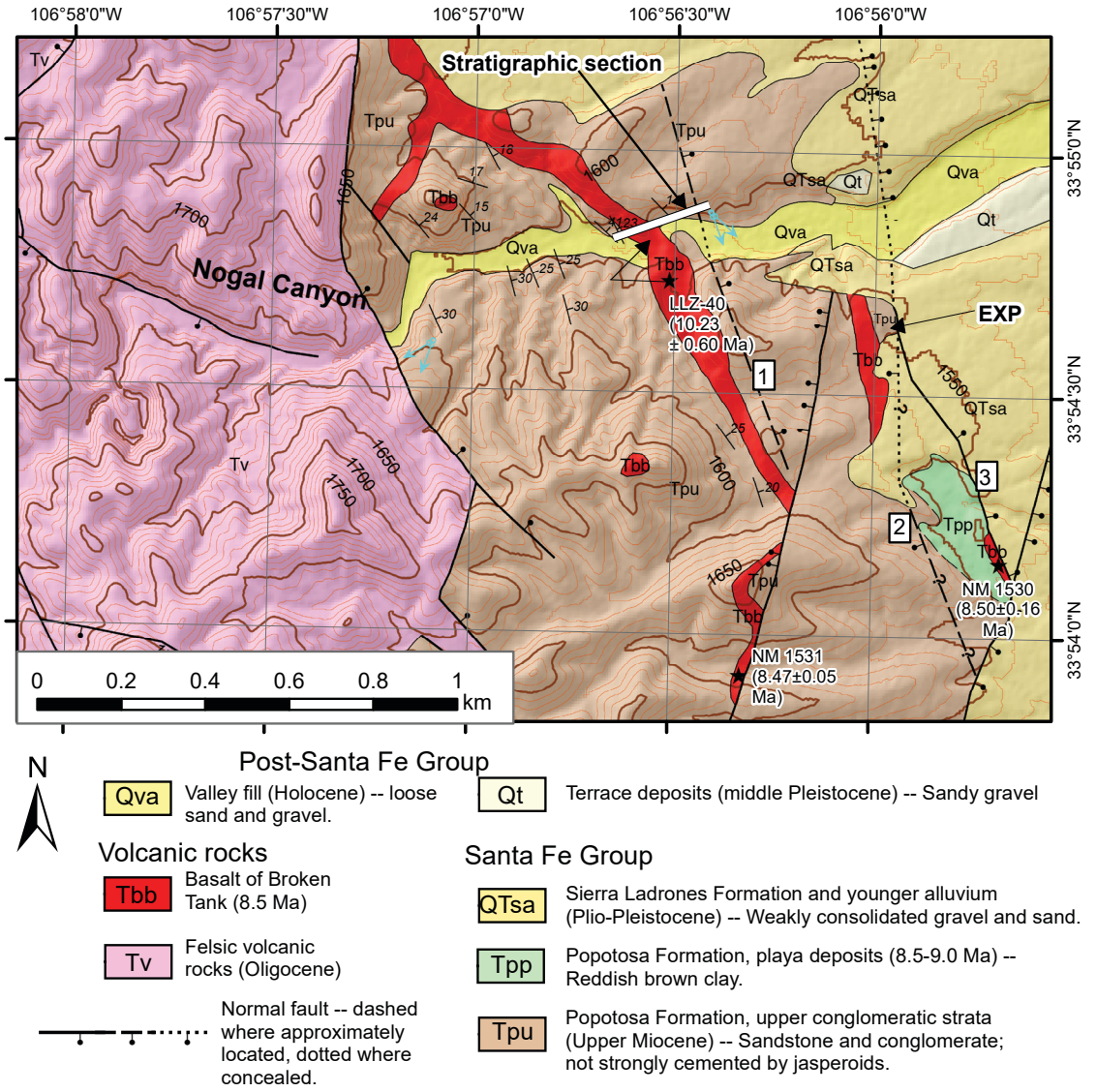

FIGURE 2. Geologic map of the study area. We measured our stratigraphic section (thick, white line) across the basalt of Broken Tank, extending downward and upward into the Popotosa Formation on either side of this basalt. Geology is simplified from Chamberlin et al. (2002), with three new faults added based on this study (labeled 1–3, inside rectangles). Two of these added faults (2 and 3) are found on either side of the playa sediment 1.5 km southeast of the stratigraphic section. Locations of three $^{40}Ar/^{39}Ar$ samples are shown as black star-shaped symbols (from Chamberlin et al., 2002, with ages updated according to a FCT monitor age of 28.201 Ma). Note the 10.23±0.6 Ma age is considered to be unreliable. Elevation contours are in meters.

southern part, divided by the Socorro lineament of Chapin (1971) that projects northeastward from the northern Chupadera Mountains to ~10–15 km due-east of Socorro. Available gravity data suggests the northern basin is asymmetric, deepening westward toward the Socorro Canyon fault system, whereas the southern basin may be more symmetrical (Fig. 1; Sanford, 1968). Near San Antonio, mapped faults bounding the southern Socorro Basin include the Socorro Canyon fault (on the west, bending in a southward direction to a southeast strike) and the Coyote and Fite Ranch faults on the east; the eastern fault system is inferred to have >500 m of east-down throw (Cather, 2005; Cather and Colpitts, 2005). Inspection of Bouguer gravity data suggests an inner graben within the southern Socorro Basin, close to the Rio Grande, that is bounded on the east by a west-down gravity gradient located ~3 km east of the river and 5–7 km west of the Fite Ranch fault (Fig. 1; also shown by Sanford, 1968). We interpret that this gravity gradient corresponds to a west-down fault that locally coincides with two short, mapped faults offsetting youngest Santa Fe Group deposits (Cather, 2005); presumably much greater vertical offset occurs at depth. Gravity data is insufficient west of the Rio Grande floodplain to infer structure, but presumably the east-tilted homocline manifested in the Chupadera Mountains continues under there.

METHODS

We focused our study to a ~100 m thick interval of conglomeratic sediment underlying and overlying the basalt of Broken Tank. A stratigraphic section was measured in this interval, on the north wall of Nogal Canyon (Fig. 2), using a Jacob staff and Abney level. Sedimentologic units were differentiated and

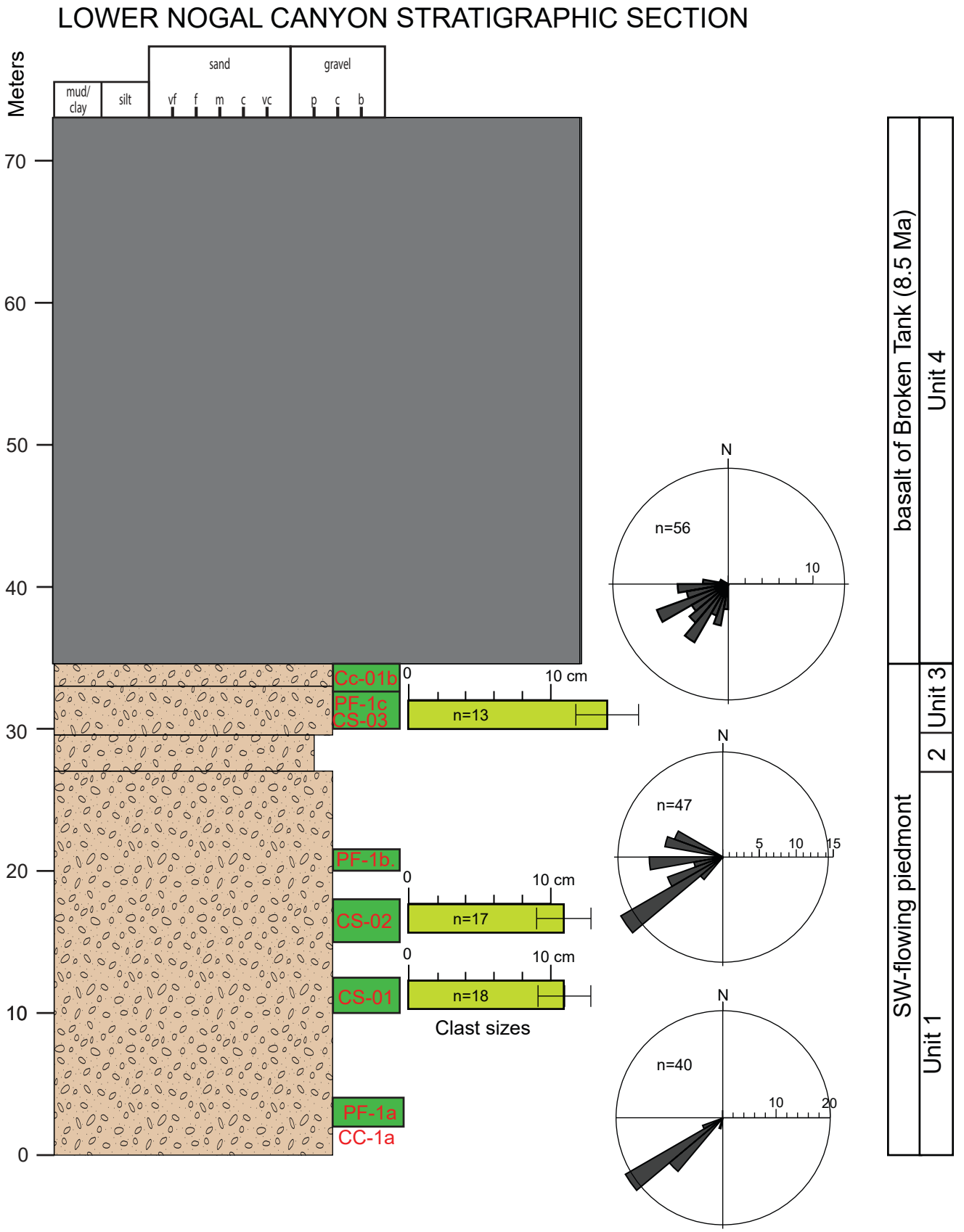

FIGURE 3. Lower part of the stratigraphic section. Interpreted depositional environment and stratigraphic unit is given on the right column. Green rectangle denotes position of sedimentologic measurements: CS-xx = maximum clast size, CC-xx = clast count, and PF-xx = paleoflow measurement (using clast imbrication). Average sizes of maximum-clast size measurements are shown in the olive-green bar graph (one standard deviation is given by the brackets; n = number of measurements). Rose diagrams show the results of paleoflow direction determined from imbricated gravel; n = number of measurements.

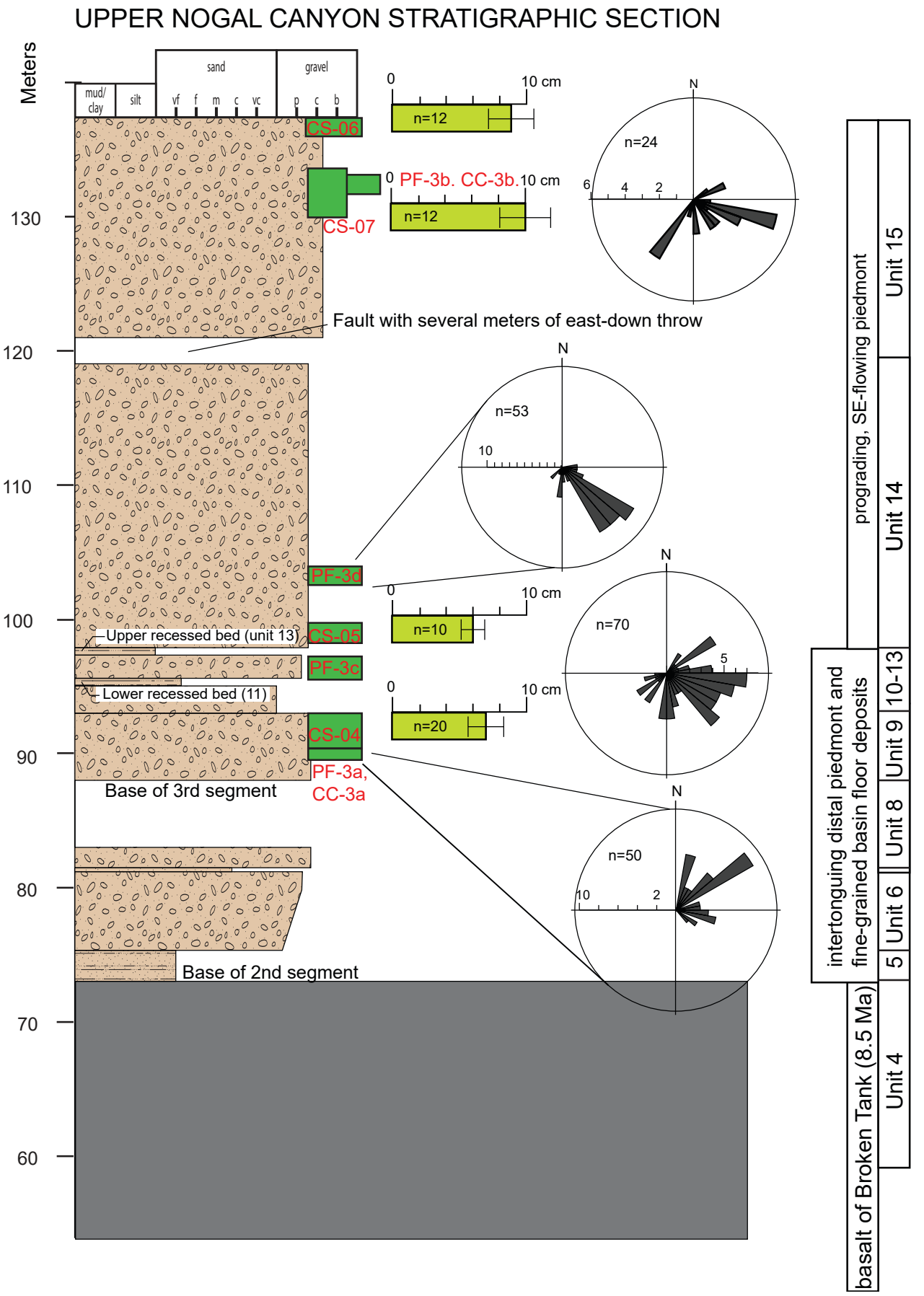

FIGURE 4. Upper part of the stratigraphic section. See Figure 3 caption for explanation of symbols.

described according to standard geologic practice (introductory paragraph of Appendix 1). Sand color and grain size were respectively measured in the field using a Munsell color chart and grain-size card.

Below the basalt we conducted clast counts at two sites (CC-1a, CC-1b), paleoflow measurements at three sites (PF-1a through PF-1c), and maximum clast size measurements at three sites (CS-01 through CS-03; Figs. 3, 4). Above the basalt, we conducted measurements at two clast count sites (CC-3a, CC-3b), four paleoflow sites (PF-3a through PF-3d), and four maximum clast size measurement sites (CS-04 through CS-07). For the clast counts, we removed clasts from moderately cemented outcrops with a rock hammer and then differentiated the clast lithologies based on features discernable

FIGURE 5. Photographs of the lower part of the stratigraphic section on the north side of Nogal Canyon. View is to the north. Top: Kevin Hobbs is standing between two west-down, minor normal faults in the lower part of unit 1 (~7.0–10.5 m). Bottom: Upper part of unit 1 (22–25.5 m). Brown box at base of outcrop is 56 cm across. In both photographs, note the tabular to lenticular beds and paucity of cross-stratification and floodplain deposits, consistent with alluvial fan facies.

with a hand lens. Clast categories were: (1) phenocryst-poor and non-foliated, felsic volcanic clasts, (2) phenocryst-poor and flow-foliated, felsic volcanic clasts, (3) moderately porphyritic, felsic volcanic clasts (5–20% phenocrysts), (4) highly porphyritic and quartz-rich, felsic volcanic clasts (20–40% phenocrysts), (5) intermediate volcanic rocks with visible plagioclase crystals ± hornblende or pyroxene phenocrysts, (6) La Jara Peak Basaltic Andesites lacking plagioclase phenocrysts and containing ≤1 mm long olivine or pyroxene phenocrysts (commonly altered to iddingsite), (7) Permian-Pennsylvanian sedimentary rocks (limestone and reddish siltstone–very fine sandstone), (8) other sedimentary clasts, and (9) jasperoid-cemented breccia or conglomerate representing reworked lower Popotosa Formation.

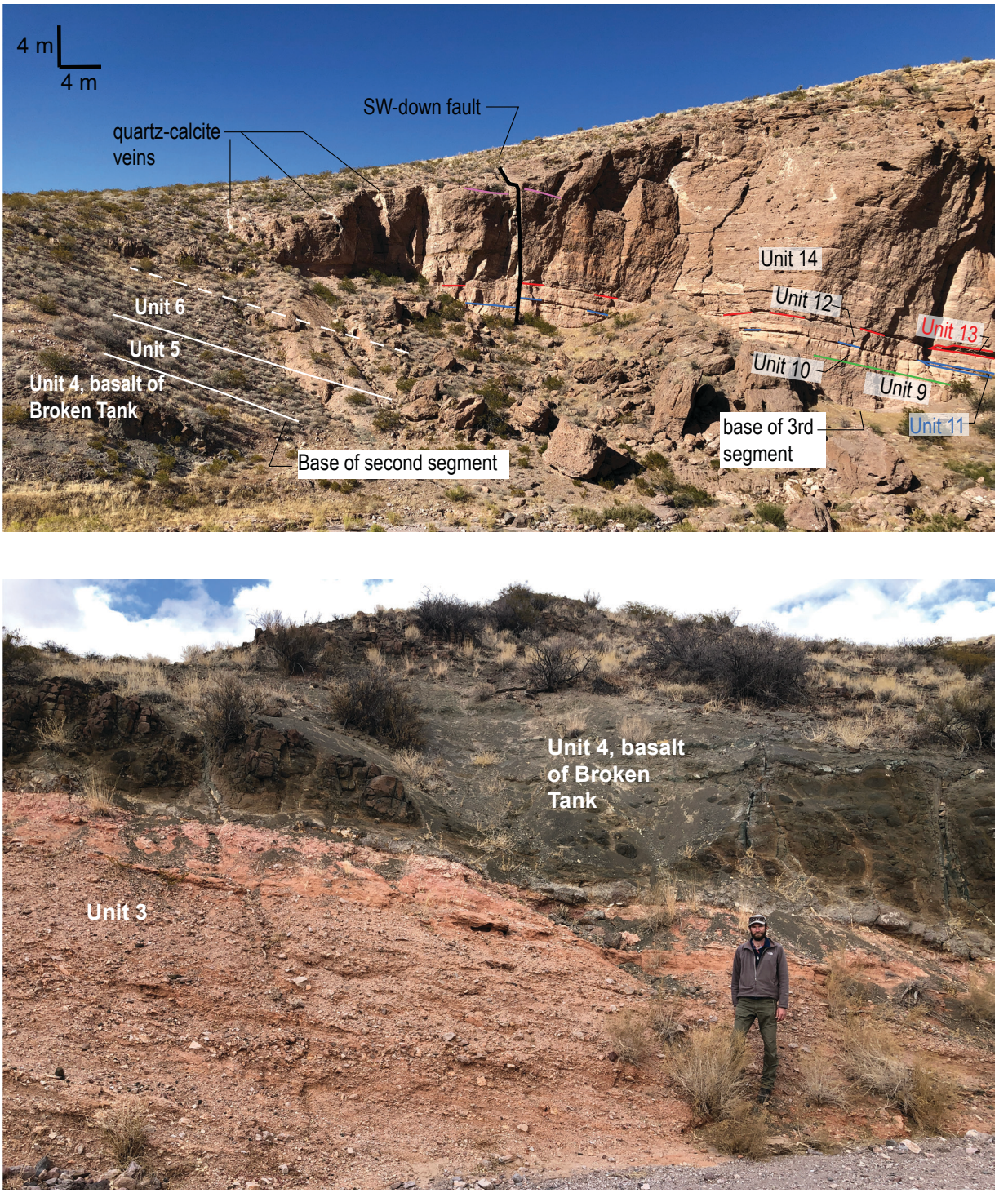

FIGURE 6. Photographs of Popotosa Formation strata immediately underlying (bottom photo) and overlying (top photo) the basalt of Broken Tank. Top: View to the northwest of the coarsening-upward, ~50 m of strata overlying the basalt; stratigraphic units are labeled per those in Figure 4 and Appendix 1. Bottom: The few meters of strata underlying the basalt of Broken Tank (top of photo) is anomalously red and has 10% cobbles. The lower stratigraphic interval remains relatively coarse until ~0.5–0.8 m below the basalt. Kevin Hobbs for scale.

A Brunton compass was used to determine paleoflow from imbricated gravel. The number of clasts measured at each site typically ranged from 40 to 56, with one site (PF-3c) having 70 measurements and another site (PF-3b) having 24 measurements. Strata below the basalt of Broken Tank dip 20–41° and required restoration of imbricated gravel back to horizontal to accurately determine paleoflow. At these sites, we measured the axis corresponding to maximum dip (plunge) and down-dip direction (bearing) of tilted clasts. Bedding orientations closest to each site were used to restore imbricated gravel positions back to horizontal using the program Stereonet (Allmendinger et al., 2012; Cardozo and Allmendinger, 2013). Paleoflow data were input as lines, with bearing (trend) being the direction of imbrication and plunge being the maximum dip value of the clast. Given that imbrication records paleoflow in the up-dip direction (i.e., opposite what we measured), we then converted our restored bearing values to paleoflow direction by adding 180°. Above the basalt of Broken Tank, strata dipped <15° and stratal tilt corrections were not performed.

The clast sizes are apparent values as seen on the roughly two-dimensional outcrop face, since the cementation of the strata made it difficult to extract the largest clasts. The long and medium axis of 10–20 individual gravel clasts were measured at each site using a ruler. The proportion of cobbles and boulders were visually estimated for each sedimentologic unit using percentage charts.

RESULTS

Stratigraphic Units

Stratigraphic section

The stratigraphic section measured in our study is presented as two parts, separated by the 40 m thick basalt of Broken Tank, which we informally refer to as the "lower part" (Fig. 3) and "upper part" (Fig. 4) of the stratigraphic section. Detailed descriptions are in Appendix 1. Clast count data are presented in Table 1 and Appendix 2, and individual measurements of clast sizes and clast imbrications are given in Appendix 2. Below the basalt (Fig. 3, units 1–3), strata consist of sandy conglomerate and subequal (±15%) pebbly sandstone that are in thin to medium, tabular to lenticular beds (Fig. 5). Pebbles comprise the majority of the gravel sizes with the rest being minor cobbles (8–10%, locally as much as 10–15%). Cobble-bearing beds are often lenticular. Gravel are subangular to angular and moderately to poorly sorted. The sandy matrix is pink (5YR 7/3), fine- to very coarse–grained, subangular, poorly sorted, and contains minor (<5%) silt-clay; the proportion of volcanic grains typically exceeds the combined amount of quartz and feldspar (as seen in hand lens). The upper 6 m (unit 3) immediately underlying the basalt exhibits a light red color (2.5YR 7/5) but lacks evidence of a paleosol (i.e., no horizonation, no calcium carbonate accumulation, no soil-related "clod" (ped) development).

There is a coarsening-upward trend in the 8.2 m of strata overlying the basalt (Fig. 4 and Appendix 1, units 5–6). The lower 2.3 m of this sequence (unit 5) is a silty very fine– to fine-grained sand (vfL-fL) that is massive, light brown, and contains trace medium to coarse sand grains. Above a gradational contact lies pebbly sand in thin, tabular beds. A coarsening-upward trend is observed where pebble content increases upwards from near-zero at the basal contact to 15% at a stratigraphic distance of 6.5 m above the basalt. Gravels are angular to subangular, poorly sorted, and sand-supported.

Above this lower coarsening-upward zone lies a 16.6 m thick interval characterized by sandy pebble-conglomerate to pebbly sandstone intercalated with fine-grained beds, the latter commonly weathering to form distinctive recesses in the outcrop (Figs. 4, 6 and Appendix 1, units 7–13). The conglomerate occurs in thin to medium, tabular to broadly lenticular beds (Fig. 7a, d). Gravel are sand- to clast-supported, subangular, and moderately to poorly sorted. There are slightly fewer cobbles (5–10%) than found in the 35 m below the basalt. The sand matrix is light reddish brown (2.5-5YR 6/4), very fine– to very coarse–grained, subangular, and has up to 1–7% silt-clay. Medium to very coarse sand is volcaniclastic. The fine-grained beds are up to 0.5 m thick, internally massive, light reddish brown (5YR 6/3), and composed of clay-silt or very fine–grained sandstone (Fig. 7c). In the fine-grained beds are trace to 5% fine to medium sand grains and trace to 0.5% coarse sand or pebbles (Fig. 7c). Some fine beds have 5–10% nodules of calcium carbonate, representing a sufficient time of surficial stability to form weak calcic soils (stage I). The lower

TABLE 1. Clast count data for the lower and upper Popotosa Formation sections at Nogal Canyon.

Clast Count (CC) Site	xl-poor* tuff/rhy (fol)	xl-poor* tuff/rhy	plag-rich int lavas	Perm sed	jasp-cmt bx/cgl	mod xl-rich* ignm	xl-rich* ignm	Tlp	other sed (non-Perm)	Tbt	n
Upper Section											
CC-3B	8.4	42.9	6.7	0.0	0.0	13.5	25.2	1.7	0.0	1.7	119
CC-3A	14.8	37.8	8.9	0.0	3.0	12.6	20.0	3.0	0.0	0.0	135
Lower Section											
CC-1B	18.3	39.7	20.6	0.0	0.0	17.5	2.4	0.8	0.8	0.0	126
CC-1A	10.3	54.0	7.1	0.0	0.8	8.7	18.3	0.8	0.0	0.0	126

NOTE: Values are percentages except for n (total number of clasts identified). Abbreviations: bx = breccia; cgl = conglomerate; cmt = cemented; fol = foliated; ignm = ignimbrite; int = intermediate; jasp = jasperoid; mod = moderately; Perm = Permian; rhy = rhyolite; sed = sedimentary; Tbt = Basalt of Broken Tank; Tlp = La Jara Peak Basaltic Andesite; xl = crystal.

*Phenocryst content definitions are as follows: crystal poor = ≤5%; moderately crystal-rich = 5–20%; crystal-rich = 20–40%.

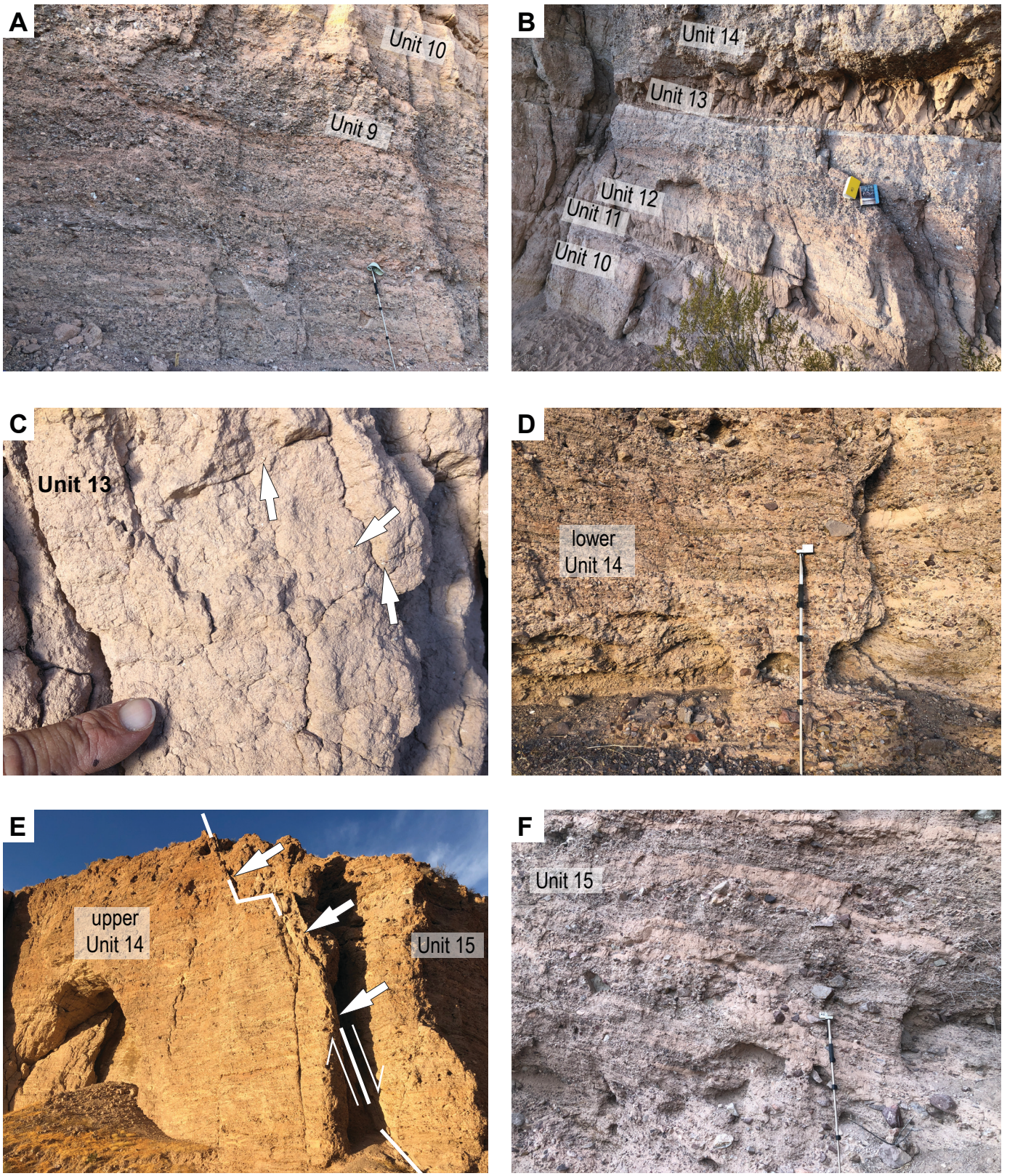

FIGURE 7. Photographs of the upper part of the stratigraphic section. (A) Tabular to broadly lenticular, thin beds of sandy conglomerate (unit 9), 1.5 m Jacob staff for scale. (B) Unit 12 (with two books) bounded by two clayey to silty, ~0.5 m thick beds (units 11 and 13); the lower 15 cm of unit 11 is gradational with the underlying unit 10 pebbly sandstone. (C) Close-up of the upper recessed marker bed (unit 13), which is a clay-silt that is massive. Trace granules (denoted by the white arrows) are found in this fine-grained matrix; these fine-grained beds are interpreted as distal run-out of hyperconcentrated flows (see Seager and Mack, 2003) as a sheetflood on a basin floor. (D) Lower part of unit 14, which has 5% interbeds of clayey-silty sand (with minor pebbles) interpreted as hyperconcentrated flows. These fine-grained beds are more common down-section in unit 14. (E) View to north of down-to-east fault zone, annotated by both heavy black lines and white arrows; we could not correlate confidently across the fault, but drag indicators are down to the east. Cliff is about ~30–36 m tall. (F) Cobble-rich strata (10–15% cobbles) near top of section at 130–134 m (unit 15), ~60 m above top of basalt; uncertain correlation across the fault in panel F means these stratigraphic heights are approximate.

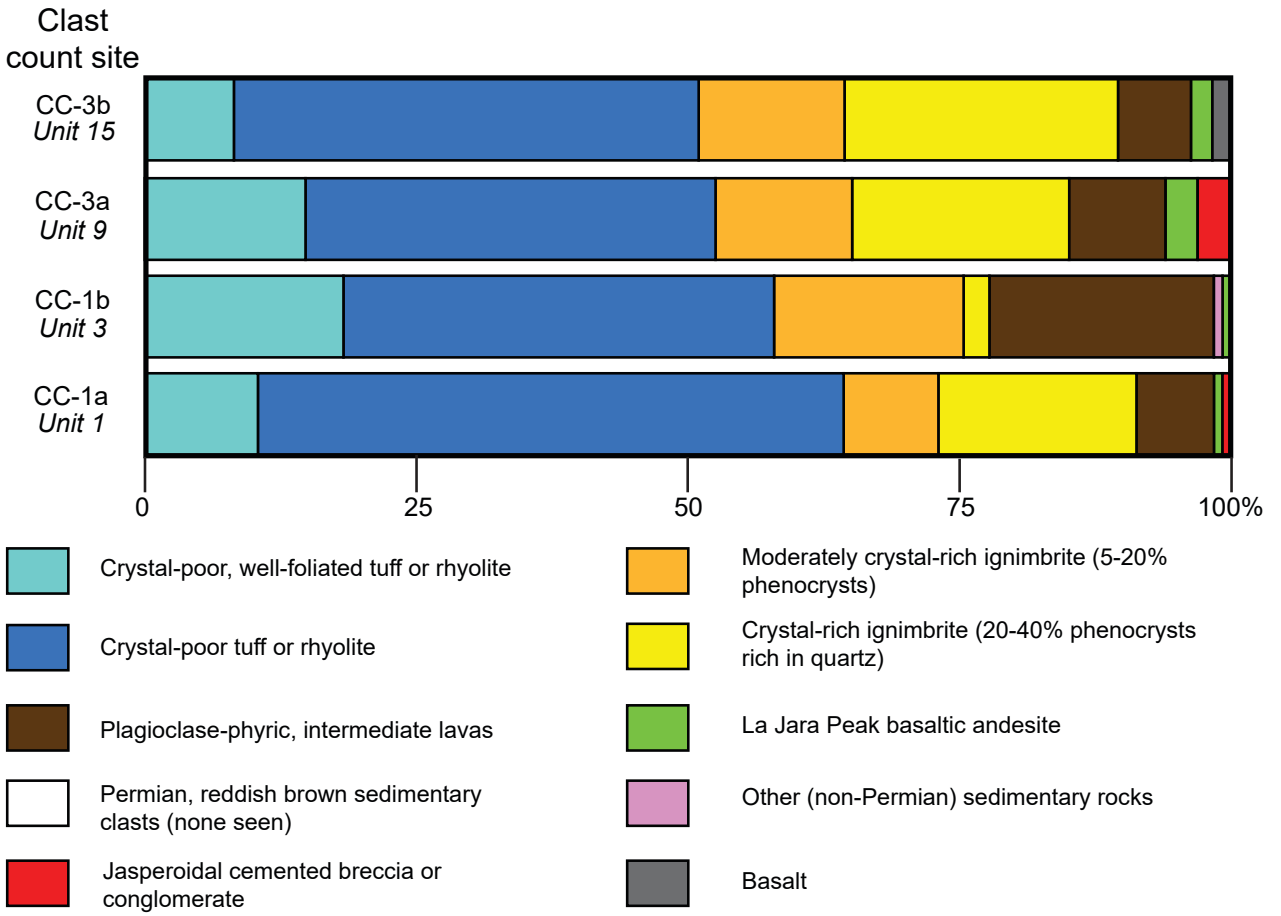

FIGURE 8. Bar charts illustrating gravel composition. Crystal-poor, felsic clasts are somewhat (by 5–10%) more common in the lower part of the stratigraphic section (units CC-1a and CC-1b). La Jara Peak Basaltic Andesite and basalt are more abundant in the Popotosa Formation above the basalt (units CC-3a and CC-3b).

contact of these fine beds can be sharp or transitional (marked by interbedding) with underlying pebbly sediment. Upper contacts are scoured. Two 0.5 m thick tabular beds composed of this fine-grained sediment make conspicuous, recessed marker beds that extend several 10s of meters across the entire upper outcrop (units 11 and 13; Figs. 4, 6, 7b).

Above the upper, thick bed of fine-grained sediment lies a >55 m thick (continuing beyond the top of our stratigraphic section), coarsening-upward interval of sandy conglomerate and pebbly sandstone (Figs. 4, 6, 7 and Appendix 1, units 14–15). The thickness is a minimum value because a north-striking, east-dipping normal fault was encountered at 120 m in the stratigraphic section (Figs. 4, 7e), probably having several meters of east-down throw. The lower 6 m of this upper unit has 5% interbeds of clayey-silty sand with minor pebbles. Bedding is very thin to medium and tabular to lenticular. Gravel is clast- to sand-supported and consists of pebbles with 3–15% cobbles (cobbles increasing in abundance up-section) that are subrounded to subangular (becoming more subrounded up-section) and poorly to moderately sorted. There is an estimated 1–3% silt-clay in the matrix. The coarsening-upward trend continues to the upper 15 m (unit 15) on the east side of the fault, which contains 1% boulders (unit 15, Figs. 4, 7f). Cobbles are commonly in lenticular, medium to thick beds, whereas pebbly sand beds are mostly very thin to thin and tabular. Sand is typically light reddish brown (5YR 6/3-4) and medium to very coarse grained, subrounded to subangular, poorly sorted, and composed of volcanic grains with 20–25% quartz and feldspar.

Exposures 1.5 km to southeast

Two stratigraphic units lying southeast of our stratigraphic section are important to consider because of their stratigraphic proximity to the basalt of Broken Tank (as mapped by Chamberlin et al., 2002). The older is located 1.5 km southeast of the upper stratigraphic section, around a cattle tank (unit Tpp in Fig. 2). This unit consists of reddish-brown clay, underlying a basalt flow a few meters thick that has been correlated to the basalt of Broken Tank (Chamberlin et al., 2002) and has returned an $^{40}Ar/^{39}Ar$ age of 8.5±0.16 Ma (updated from Chamberlin et al., 2002, using a FCT monitor age of 28.201 Ma). The other unit lies superjacent to the basalt at a distance of 1 km southeast of the upper stratigraphic section ("EXP" in Fig. 2). This upper unit is composed of light reddish-brown, interbedded clay, sand, and pebbly sand subjacent to the basalt of Broken Tank (as mapped by Chamberlin et al., 2002).

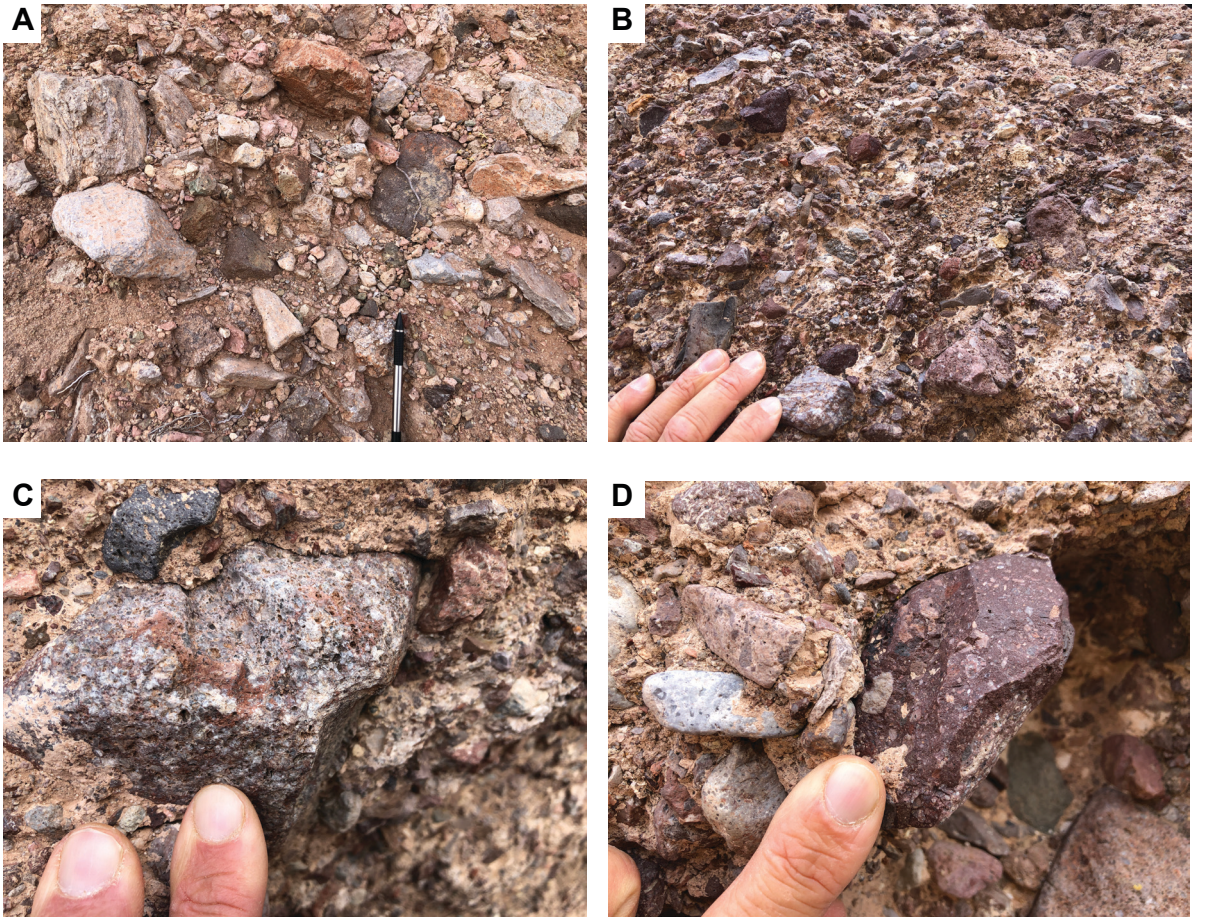

FIGURE 9. Close-up photographs of gravel composition. (A) Subangular pebbles and cobbles in unit 1, which was sourced to the northeast. This unit had high amounts of crystal-poor rhyolite similar to that seen in the upper moat facies of the Luis Lopez Formation. (B) Subrounded-subangular gravel of unit 14 in a modern-day, meter-scale fall block (from unit 14); paleocurrent data from in situ unit 14 indicate this unit was sourced to the northwest (Fig. 4). Note the overall darker color of the clasts and slightly more rounded gravel compared to the A panel. (C) Reddish-brown, swirly, and somewhat flattened dacite clots in a very coarse pebble of phenocryst-rich upper Lemitar Tuff. These types of clasts have not been observed east of the Rio Grande, but are common in the Lemitar Tuff of the eastern Magdalena Mountains (Chamberlin et al., 2002; Osburn et al., 1981). (D) Reddish-brown, jasperoidal-cemented clast of lower Popotosa Formation. This type of clast matches with those seen in the northern Chupadera Mountains. The photographs of panels C and D were from a block of cemented sediment that tumbled down from a ledge of unit 14.

Clast Sizes

The average and standard deviation of the medium (b axis) of the gravel are plotted on Figures 3–4, with the raw data tabulated in Appendix 2. The average size at each site is mostly 9–11 cm. Particularly coarse gravel was measured a few meters below the basalt (averaging 14 cm at site CS-03). For the interval above the basalt, the lower two sites (CS-04 and CS-05 in units 9 and 14, respectively) have finer b axes (6–7 cm average) than the upper two sites (CS-06 and CS-07, 9–10 cm average), consistent with the upward-coarsening trend seen in the upper part of the stratigraphic section.

Clast Composition

Gravel composition data is listed in Table 1 and presented as bar graphs in Figure 8. Superficially, there is a difference in color and a slight difference in rounding between the gravel in the Popotosa Formation below the basalt and above the basalt, with the gravel above being slightly more rounded (especially up-section in unit 14) and darker above the basalt (compare gravel in Fig. 9a and 9b). However, only minor differences were noted in our clast counts (Fig. 8, Table 1). The gravel at all four clast-count sites are composed of felsic volcanic gravel with minor plagioclase-phyric intermediate volcanic gravel. The proportion of intermediate clasts is typically 6–9%, but at clast-count site CC-1b (18–19 m below the basalt), there is an anomalously high proportion (21%) of these clast types. We did not observe any reddish siltstones or very fine sandstones that would potentially correlate to a source area underlain by the Permian Abo or Meseta Blanca formations. “Other” sedimentary rocks were also conspicuously absent. Jasperoid-cemented breccia or conglomerates were absent or very sparse (1%), with the most (3%) being found 17–18 m above the basalt (Table 1 and Fig. 8, CC-3a, Fig. 9d). La Jara Peak basaltic clasts appear to be more abundant above the basalt (2–3% in CC-3a and CC-3b) compared to below the basalt (<1% in CC-1a and CC-1b). At a distance ~60 m above the basalt in our stratigraphic section, at site CC-3b, we note two basalt clasts that may represent fluvially reworked basalt of Broken Tank.

A slight difference in the gravel below and above the basalt of Broken Tank is the proportion of crystal-rich and moderately crystal-rich tuffs vs. crystal-poor tuffs (foliated and non-foliated), and the nature of the crystal-poor tuffs. Crystal-rich and moderately crystal-rich tuffs comprise 20–27% of the clast population below the basalt and 32–39% above the basalt. Crystal-poor tuffs comprise 58–64% below the basalt and 52–53% above the basalt. A qualitative observation of up-section gravel differences was made by co-author RMC, an expert on the Luis Lopez Formation (Chamberlin, 1999; Chamberlin et al., 2002, 2004), who interprets that fine-grained rhyolites similar to "moat-fill rhyolites" of the Luis Lopez Formation constitute a majority of the crystal-poor tuffs below the basalt and are less abundant above the basalt.

Another noteworthy difference is the sparse presence of clasts of a distinctive type of upper Lemitar Tuff above the basalt (Fig. 9c) and its apparent absence below it. This clast type is characterized by being rich in quartz phenocrysts and exhibiting reddish brown, swirly fragments of flattened dacite "clots" (Fig. 9c). These dacite clots are not present in the upper Lemitar Tuff in the Socorro Mountains and east of the Rio Grande, but are abundant in the Lemitar Tuff of the eastern Magdalena Mountains (Chamberlin, 1999; Chamberlin et al., 2002; Chamberlin and Osburn, 2006). This key clast type was observed in meter-scale fall blocks on the canyon floor that originated from unit 14.

Paleoflow

Paleoflow data are plotted on rose diagrams with 10° bin size (Figs. 3–4). Of three quantitative datasets (clast sizes, gravel composition, paleoflow), paleoflow shows the most difference above and below the basalt of Broken Tank. Below the basalt, paleoflow was to the southwest, whereas above the basalt it was generally to the southeast. The lowest paleoflow site in the upper part of the section, PF-3a (18–19 m above the basalt of Broken Tank), is the sole site in the upper part of the section that exhibits an average northeast-directed paleoflow. In the topmost paleoflow measurement (PF-3b), there was a relatively wide dispersion of directions, with 5 clasts showing a southwest direction, 3 a northeast direction, and the majority (17) indicating a southeast-directed paleoflow.

DISCUSSION

Depositional Environments

We are confident that the gravelly sediment seen in the majority of the stratigraphic section was deposited in an alluvial fan or piedmont depositional environment. Beds are mostly thin to medium and tabular to broadly lenticular. Sparse lenticular beds, including most beds containing cobbles, probably represent the basal parts of paleochannel fills. Cross-stratification is very rare. We infer a large component of high-energy sheetflooding to produce the broad, coarse-grained beds. Conspicuously absent are cross-stratified, sandy-gravelly channel fills (potentially displaying fining-upward trends) and adjoining floodplain deposits associated with potential fluvial environments. Paleoflow (and paleo-slope) in the piedmont deposits below the basalt of Broken Tank was to the southwest, and paleoflow (paleo-slope) of the piedmont deposits above the basalt was dominantly southeast (locally northeast).

In the upper part of the stratigraphic section, there is a robust coarsening-upward trend consistent with a prograding piedmont. The most dramatic coarsening occurs in the upward increase in pebbles seen in unit 6 (Fig. 4). The middle to upper units (units 9–15 in Fig. 4) also exhibit a coarsening-upward trend, as reflected by the increase in cobble proportion (3–10% to 10–15%, Appendix 1) and maximum clast sizes (6–7 cm to 9–10 cm; Fig. 4, Appendix 2). We do not have enough data in the lower part of the section to confidently assess coarsening- versus fining-upward trends.

The lower part of the upper interval, extending 25 m above the top of the basalt of Broken Tank (between 73–98 m in the stratigraphic section), is interpreted as distal piedmont deposits intertonguing with fine-grained basin floor facies, the latter including eolian deposits (Fig. 4). The basin-floor deposits are interpreted for the tabular, laterally extensive beds composed of silt-clay mixed with very fine–lower to fine–lower sand. The lowest 2.3 m of the upper section (unit 5, at 73.0–75.3 m; Fig. 4) is likely eolian sediment due to its well-sorted, fine-grained texture of silt through fine-grained sand and lack of pebbles; the paucity of volcanic lithic grains in this unit also is consistent with eolian sand transported from a relatively distant, low volcanic-composition source area different from the volcanic-rich sand composing the local piedmont deposits. Furthermore, comparison with younger (Quaternary) basalt flows in south-central New Mexico indicates that accumulation of fine-grained eolian deposits can be expected on top of a basalt. Rough surfaces of late Pleistocene basaltic lava flows have been postulated as effective traps of windblown sediment at Amboy crater and in the Cima volcanic field in the Mojave Desert of southern California (Greeley and Iversen, 1981; Wells et al., 1985).

In the higher fine-grained beds, such as the two recessed marker beds, there are trace pebbles, and the lower recessed bed (unit 11) has a transitional, interbedded contact with underlying pebbly sandstone. These stratigraphically higher fine-grained beds are more likely alluvial than eolian and interpreted to have been deposited by sheetflooding debouching from channel mouths on the distal piedmont. These are inferred to be associated with a gently sloping basin floor located east-southeast of the southeast-sloping piedmont. Because of the gradational, upward-coarsening nature of the contact between units 5 and 6, it is inferred that the upper part of unit 5, although probably eolian, also represents deposition on the eastern margin of the basin floor that was then gradually encroached upon by a southeastward-prograding, distal piedmont (unit 6).

The Popotosa Formation exposures 1.0–1.5 km to the southeast of the upper stratigraphic section, adjoining the basalt of Broken Tank, are interpreted to belong to a small, isolated playa adjoining a distal piedmont environment. The playa (Tpp on Fig. 2) is characterized by several meters of reddish-brown clays that must have been deposited in a low-en-

ergy environment. The possible depositional environments for this fine-grained sediment include: (1) part of a larger playa, although it would appear to be a separate playa than the large one to the north (Fig. 10); (2) a relatively localized playa controlled by hanging wall subsidence along a fault (e.g., Love et al., this volume); or (3) impoundment of flow against a slightly older basalt flow. We favor the latter hypothesis, but further geochemistry is needed to test it. As an argument against the second possibility, this location is not obviously located in a hanging wall of a major fault (Fig. 2). The sediment above the basalt ("EXP" on Fig. 2) reflects deposition on the margin of a basin floor and distal piedmont.

Paleogeographic Changes

We interpret a major paleogeographic change that occurred a short time after the emplacement of the 8.5 Ma basalt of Broken Tank (Fig. 10). Before 8.5 Ma, there was a southwest-sloping piedmont whose source area had a high proportion of crystal-poor rhyolites similar to those seen in the upper Luis Lopez Formation (Socorro caldera-fill). Jasper-cemented breccias (conglomerates) clasts are very sparse to absent and no western-provenance, upper Lemitar Tuff clasts are present. Luis Lopez Formation rhyolites were likely thickest within the former Socorro caldera, whose eastern boundary likely extended close to the modern-day Rio Grande (Figs. 1, 10; Chamberlin et al., 2004, fig. 2). Because of the relative abundance of crystal-poor rhyolite gravel in the lower part of the stratigraphic section, we interpret that there may have been a paleotopographic high, possibly exceeding 100s of meters in relief, somewhere in the vicinity of the modern-day community of Luis Lopez (Fig. 10). The relatively coarse texture of the conglomerate in the lower part of the section is consistent with a relatively close source area. However, the gravel of the lower part of the section is sufficiently diverse that there was probably contribution by drainages sourced farther eastward in what is now the southern Quebradas (Fig. 10), consistent with the inferred source of the southwest-flowing piedmont units of Cikoski (2010) near the Bosque del Apache National Wildlife Refuge headquarters. The absence of Pennsylvanian-Permian clasts indicate that the middle-southern Quebradas were covered by a blanket of volcanic rocks and/or volcaniclastic sediment.

After 8.5 Ma, there is evidence of an intertonguing distal piedmont with an adjacent basin floor to the east (Fig. 4, units 5–13). This later piedmont generally sloped to the southeast based on our paleoflow data. Early in this period, local piedmont deposition may have been dominated by an alluvial fan centered southwest of our study area, producing northeast-directed paleoflow at clast count site CC-3a. With time, the southeast-flowing piedmont (coalesced alluvial fans) and adjoining basin floor prograded east-southeast.

In addition to southeastward paleoflow, the presence of Magdalena Mountain–provenance upper Lemitar Tuff clasts (with dacite clots) and the slightly higher proportion of jasperoid-cemented breccia clasts (Fig. 9) are consistent with a source area to the northwest. We interpret that the latter piedmont was sourced mainly on the eastern slope of the Magdalena Mountains, which based on thermochronologic data (Abbey and Niemi, 2020) were being rapidly uplifted between ~19 to 15 Ma (long-term rates of 0.5 mm/yr, decreasing to 0.2 mm/yr from 15 to 0 Ma); therefore, the Magdalena Mountains were probably higher than the low bedrock hills characterizing the northern Chupadera Mountains. As noted above, the crystal-rich, upper Lemitar Tuff featuring dacite clots has not been found east or southeast of Socorro, and is relatively sparse in the Chupadera Mountains.

The age of the upper, southeast-sloping piedmont is interpreted to be latest Miocene. The maximum age is constrained by the age of the basalt of Broken Tank. The appreciable thickness of the basalt of Broken Tank, measured as 40 m at the study site, would have impeded deposition here for some time after its emplacement. Exactly how long deposition ceased is not constrained at the site, but we do note that on the west side of the Chupadera Mountains, ~20 m of Popotosa Formation strata are present between the 9.80±0.05 Ma basalt of Chupadera Spring and the 8.5 Ma basalt of Broken Tank (Chamberlin et al., 2002; both flows are shown on Fig. 1), giving a sedimentation rate of roughly 20 m per 1.3 my, or 40 m per ~2.5 my, that may be loosely applicable to our study site on the east side of the Chupadera Mountains. Therefore, a hiatus in deposition of ~1–2 my after the 8.5 Ma emplacement of the basalt of Broken Tank is not unreasonable. We argue that the post-basalt deposit is latest Miocene rather than Pliocene in age because of its reddish color, 10–13° stratal tilts, and local presence of quartz + calcite veins (Fig. 6, top photo); the latter suggests that the sediment predated a manganese-calcite hydrothermal alteration event at 6.4–6.5 Ma (Lueth et al., 2004). In contrast, mapped Plio-Pleistocene strata of the Sierra Ladrones Formation near the study area is buff-colored, typically dips <5°, and lacks quartz-calcite veins.

Post 8.5 Ma Change in Rift Tectonic Activity

Given our interpreted age for the upper part of the stratigraphic section and the age of the basalt of Broken Tank, we argue that a major tectonic change occurred in the southern Socorro Basin and Chupadera Mountains between 8.5 Ma and 6.5 Ma. This tectonic change resulted in major subsidence of the paleotopographic high inferred for the Luis Lopez area and the former southwest-flowing piedmont. Faults controlling this subsidence may possibly correspond to the west-down Bouguer gravity anomaly gradient located approximately a few km east of the modern-day Rio Grande (Fig. 1). The postulated fault zone along this Bouguer gradient has poor expression in the late Quaternary geologic record (compare Fig. 1 with maps in Personius and Jochems, 2016). The maximum age for this subsidence is between the 8.5 Ma age of the basalt of Broken Tank and the inferred age of the base of the upper piedmont unit (7–8 Ma). By roughly 7.5–6.5 Ma, enough subsidence occurred in this graben to induce eastward migration of the basin floor to what is now the Rio Grande floodplain, concomitant with east-southeast progradation of the younger piedmont.

Tilting of fault-bounded, tectonic blocks created basins and an early version of the Chupadera Mountains before 8.5

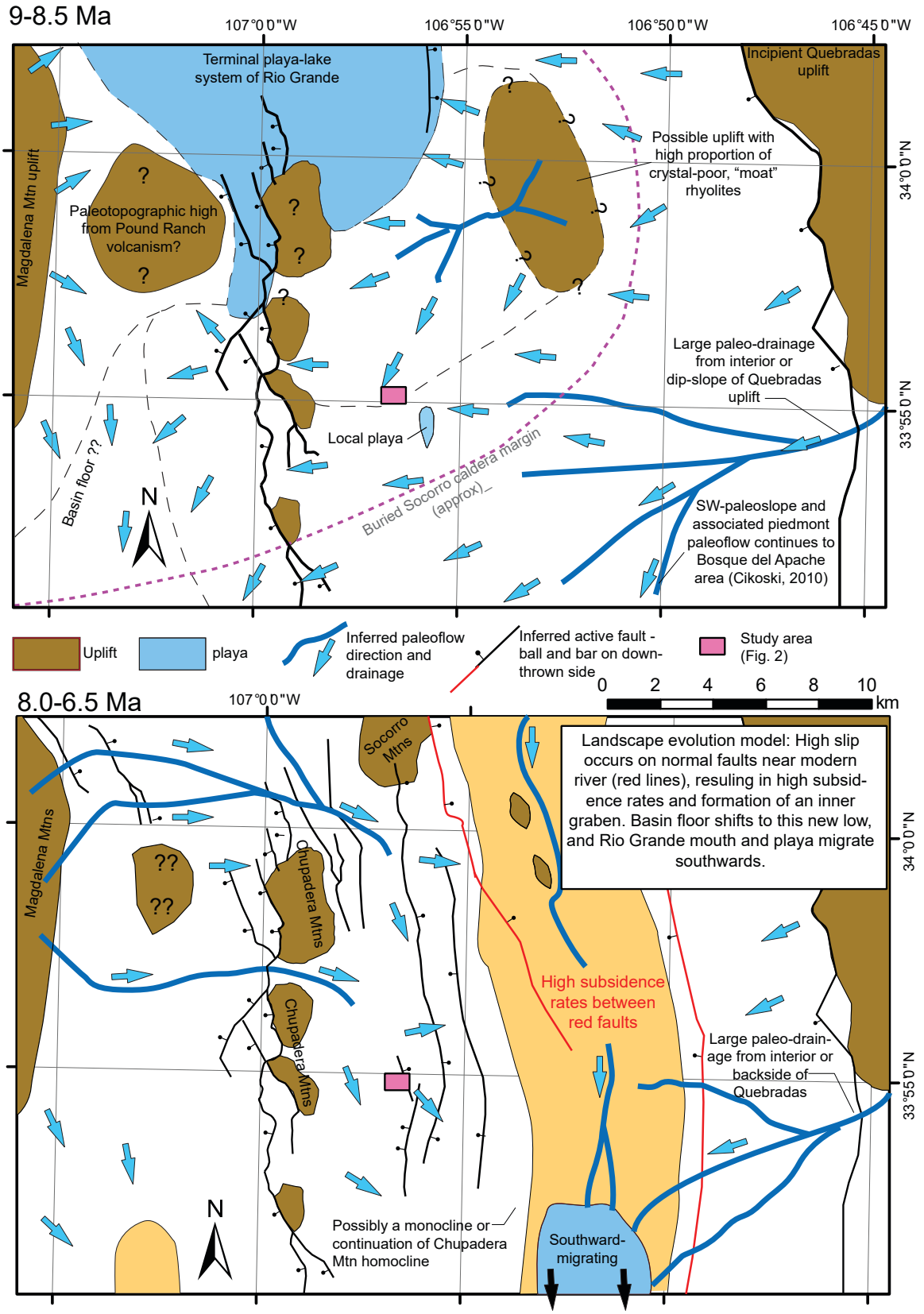

FIGURE 10. Interpretative paleogeographic maps for 9.0–8.5 Ma (top) and 8.0-6.5 Ma (bottom), illustrating the replacement of the southwest-sloping, northeast-provenance piedmont at the study area (pink box) with a southeast-sloping, northwest-provenance piedmont. Thin black lines are boundaries between paleogeographic elements, including piedmont systems sourced from unique areas. Thick black lines are faults, with the ones near the center of the basin colored red. These panels encompass the time period before and after the emplacement of the 8.47±0.05 Ma basalt; note that we do not show a time panel for the basalt and paleogeography at 8.47 Ma. Our preferred interpretation for this reversal is a concentration of strain along faults near the center of the Socorro Basin, particularly a postulated fault corresponding with a high Bouguer anomaly gradient a few kilometers east of the modern-day Rio Grande.

Ma (Chamberlin et al., 2002). This is evidenced by two bedrock-incised paleovalleys near the crest of the mountains that are back-filled by Popotosa conglomeratic sediment, with interpreted westward paleoflow, capped by the 8.5 Ma basalt of Broken Tank or the 9.8 Ma basalt of Chupadera Spring. Slip continued on the western-bounding fault of these mountains, the west-down Chupadera fault, after 8.5 Ma, based on the 210 m of vertical displacement of the basalt of Broken Tank across three Chupadera fault strands at a location ~2 km north-northwest of the west end of the main narrows of Nogal Canyon (measuring from the geologic maps of Osburn et al., 1981, and Chamberlin et al., 2002). East-down tilting, likely accompanying faulting on the west-down Chupadera fault, continued after 8.5 Ma, because post-8.5 Ma Popotosa Formation strata in the study area are tilted eastward 5–14°.

The apparent eastward shift in extensional strain to the present-day Socorro Basin corresponds temporally with three tectonic phenomena in the Rio Grande rift. One, this shift is consistent with the long-term decrease in exhumation rates of the Magdalena Mountains that occurred after 15 Ma (Abbey and Niemi, 2020, Fig. 3). Two, the major reorganization of extensional strain and basin geometry interpreted here also occurred at the same time in the southern Caballo Mountains and Rincon-Hatch Basins (Seager and Mack, 2003; Mack et al., 1994). Three, inward shifting of strain occurred during the late Miocene for the Santo Domingo–Española Basin area (Gardner and Goff, 1984; Baldridge et al., 1994; Smith, 2004; Minor et al., 2006, 2013; Koning et al., 2013). In the Española Basin, such a shift in rift strain could have been influenced by magmatism related to the Jemez volcanic field, and 11–7 Ma magmatism in the Socorro area (Chamberlin, 1999; Chamberlin et al., 2002; Bobrow et al., 1983; Newell, 1997) also could have influenced local fault activity.

Implications for Rio Grande Evolution

Previous models explaining the southward integration of the Rio Grande, such as epeirogenic uplift of the San Luis Basin and surrounding Rocky Mountains (Kottlowski, 1953; Repasch et al., 2017) or decreases in tectonic subsidence rates (Connell et al., 2005) only consider the headwaters or middle flow-reaches of the river. The paleogeographic changes documented by the exposures in Nogal Canyon add a potential downstream driver to Rio Grande integration. Namely, significant post-8.5 Ma subsidence of a previous topographic high and piedmont slope in what is now the Rio Grande Valley, near Luis Lopez and San Antonio, induced the basin floor facies, presumably including the aforementioned playa, to migrate to the south-southeast. In other words, tectonic subsidence lowered the southeastern part of the sill that confined the terminal playa to the Socorro region. Concurrent work documents high rates of slip along a possible continuation of faults bounding the east side of the "inner Socorro Basin graben," 20 km south of our study area (Koning and Heizler, this volume). Collectively, the high fault slip rates and subsidence of the "inner Socorro Basin graben" allowed the playa and eventually the Rio Grande to off-lap into the area of maximum subsidence, eventually creating a paleotopographic-low pathway for the ancestral Rio Grande to extend southwards into the San Marcial Basin. The integration of the Socorro Basin may have occurred by 6.5–7.0 Ma, considering the 6.97±0.02 Ma age of the Sedillo Hill basaltic andesite that caps playa deposits northwest of the Chupadera Mountains (Chamberlin and Osburn, 2006). After occupying the central Socorro Basin for 3–4 my, the Socorro terminal playa was no more, and the Rio Grande kept on flowing southward.

However, this study alone cannot negate an alternative hypothesis: that increased sediment and/or water discharge delivered from the Rio Grande, perhaps due to paleoclimatic and paleoclimatic-modulated erodibility changes in the paleo-landscape, caused the Socorro Basin to fill up rapidly with sediment or water. This rapid "filling up," either by water or sediment, would have facilitated over-topping of the southern sill. Such a paleoclimatic driver would have operated independently of the aforementioned tectonic driver, and both could have been occurring at the same time. This hypothesis is currently being examined by sedimentologic work the lead author is conducting on the playa and fluvio-deltaic sediment of the late Miocene playa lake near the northern Chupadera Mountains.

CONCLUSION

Our paleoflow data, in agreement with clast-count data, indicate that a major paleogeographic change occurred in the 1–2 my following emplacement of the 8.5 Ma basalt of Broken Tank. A southwest-sloping piedmont, whose toe extended >2 km west of the west side of the Chupadera Mountains, was replaced by a southeast-flowing piedmont with a basin floor centered near the modern Rio Grande floodplain. We postulate that this change occurred in response to an eastward shifting or concentration of extensional strain to an eastern fault bounding an "inner Socorro Basin graben," whose location corresponds to a steep Bouguer gravity gradient (Sanford, 1968). By ca. 6.5–7.0 Ma, what was once a medial piedmont, perhaps containing a bedrock paleotopographic high, was converted to a basin floor, allowing the ancestral Rio Grande to flow southward into the adjoining San Marcial Basin. Thus, the latest Miocene extensional tectonic reorganization observed to the south near the southern Caballos Mountains (Mack et al., 1994) also occurred in the Socorro area, and this tectonic change was an important initial driver for the southward integration of the ancestral Rio Grande. This could have happened in conjunction with upstream paleoclimatic fluvial-integration drivers, a hypothesis that is currently being examined.

ACKNOWLEDGMENTS

Based on reconnaissance work, Dr. Steven Cather (NMBGMR) was the first to suspect a notable change in piedmont deposits across the basalt of Broken Tank in lower Nogal Canyon, accompanied by a change in paleoflow direction. He suggested to the lead author to undertake a more detailed study. Claire and Adele Koning assisted in collecting maximum clast sizes in the stratigraphic section. Marissa Fischera provided

complete Bouguer anomaly gravity data (point data and contours). The manuscript was improved by the helpful reviews of Steven Cather, Jacob Thacker, and Geoff Rawling.

REFERENCES

Abbey, A.L., and Niemi, N.A., 2020, Perspectives on continental rifting processes from spatiotemporal patterns of faulting and magmatism in the Rio Grande rift, USA: Tectonics, v. 39, e2019TC005635, https://doi.org/10.1029/2019TC005635.

Allmendinger, R.W., Cardozo, N., and Fisher, D.M., 2012, Structural Geology Algorithms: Vectors and Tensors: Cambridge, Cambridge University Press, 302 p.

Armstrong, C., Dutrow, B.L., Henry, D.J., Thompson, R.A., 2013, Provenance of volcanic clasts from the Santa Fe Group, Culebra graben of the San Luis Basin, Colorado: A guide to tectonic evolution, *in* Hudson, M.R., and Grauch, V.J.S., eds., New Perspectives on Rio Grande Rift Basins: From Tectonics to Groundwater: Geological Society of America, Special Paper 494, p. 21–45, doi: 10.1130/2013.2494(02).

Baldridge, W.S., Ferguson, J.F., Braile, L.W., Wang, B., Eckhardt, K., Evans, D., Schultz, C., Gilpin, B., Jiracek, G.R., and Biehler, S., 1994, The western margin of the Rio Grande rift in northern New Mexico: An aborted boundary?: Geological Society of America Bulletin, v. 106, p. 1538–1551, doi:10.1130/0016-7606(1994)106<1538:TWMOTR>2.3.CO;2.

Bobrow, D.J., Kyle, P.R., and Osburn, G.R., 1983, Miocene rhyolitic volcanism in the Socorro area of New Mexico: New Mexico Geological Society, Guidebook 35, p. 211–217.

Cardozo, N., and Allmendinger, R.W., 2013, Spherical projections with OSX-Stereonet: Computers & Geosciences, v. 51, p. 193–205.

Cather, S.M., 2005, Geologic map of the San Antonio 7.5-minute quadrangle: New Mexico Bureau of Geology and Mineral Resources, Open-file Geologic Map 58, scale 1:24,000.

Cather, S.M., and Colpitts, R., Jr., 2005, Geologic map of the Loma de las Cañas 7.5-minute quadrangle: New Mexico Bureau of Geology and Mineral Resources, Open-file Geologic Map 110, scale 1:24,000.

Cather, S.M., and Read, A.S., 2003, Geologic map of the Silver Creek 7.5-minute quadrangle: New Mexico Bureau of Geology and Mineral Resources, Open-file Digital Geologic Map OF-GM 075, scale 1:24,000.

Cavazza, W., 1986, Miocene sediment dispersal in the central Espanola Basin, Rio Grande rift, New Mexico, USA: Sedimentary Geology, v. 51, p. 119–135, doi:10.1016/0037-0738(86)90027-8.

Chamberlin, R.M., 1999 (rev. 2022), Geologic map of the Socorro 7.5-minute quadrangle: New Mexico Bureau of Geology and Mineral Resources, Open-file Geologic Map 34, scale 1:24,000.

Chamberlin, R.M., and Cikoski, C.T., 2010, Geologic map of the Indian Well Wilderness quadrangle, Socorro County, New Mexico: New Mexico Bureau of Geology and Mineral Resources, Open-file Geologic Map 201, scale 1:24,000.

Chamberlin, R.M., and Osburn, G.R., 2006, Geologic map of the Water Canyon quadrangle, Socorro County, New Mexico: New Mexico Bureau of Geology and Mineral Resources, Open-file Geologic Map 118, scale 1:24,000.

Chamberlin, R.M., Eggleston, T.L., and McIntosh, W.C., 2002, Preliminary geologic map of the Luis Lopez 7.5-minute quadrangle: New Mexico Bureau of Geology and Mineral Resources, Open-file Geologic Map 53, scale 1:24,000.

Chamberlin, R.M., McIntosh, W.C., and Eggleston, T.L., 2004, $^{40}Ar/^{39}Ar$ geochronology and eruptive history of the eastern sector of the Oligocene Socorro caldera, central Rio Grande rift, New Mexico: New Mexico Bureau of Geology and Mineral Resources, Bulletin 160, p. 251–279.

Chapin, C.E., 1971, The Rio Grande rift, Part I: Modifications and additions: New Mexico Geological Society, Guidebook 22, p. 191–201.

Chapin, C.E., 2008, Interplay of oceanographic and paleoclimate events with tectonism during middle to late Miocene sedimentation across the southwestern USA: Geosphere, v. 4, no. 6, p. 976–991, doi:10.1130/GES00171.1.

Cikoski, C.T., 2010, Geology of the Neogene basin fill on the Indian Well wilderness 7.5' quadrangle, central Rio Grande rift, New Mexico [M.S. thesis]: Socorro, New Mexico Institute of Mining and Technology, 160 p.

Connell, S.D., Koning, D.J., and Cather, S.M., 1999, Revisions to the stratigraphic nomenclature of the Santa Fe Group, northwestern Albuquerque Basin, New Mexico: New Mexico Geological Society, Guidebook 50, p. 337–353.

Connell, S.D., Hawley, J.W., and Love, D.W., 2005, Late Cenozoic drainage development in the southeastern Basin and Range of New Mexico, southeasternmost Arizona, and western Texas, *in* Lucas, S.G., Morgan, G.S., and Zeigler, K.E., eds., New Mexico's Ice Ages: New Mexico Museum of Natural History and Science, Bulletin 28, p. 125–150.

Connell, S.D., Smith, G.A., Geissman, J.W., and McIntosh, W.C., 2013, Climatic controls on nonmarine depositional sequences in the Albuquerque Basin, Rio Grande rift, north-central New Mexico, *in* Hudson, M.R., and Grauch, V.J.S., eds., New Perspectives on Rio Grande Rift Basins: From Tectonics to Groundwater: Geological Society of America, Special Paper 494, p. 383–425, doi:10.1130/2013.2494(15).

Eggleston, T.L., 1982, Geology of the central Chupadera Mountains, Socorro County, New Mexico [M.S. thesis]: New Mexico Bureau of Mines and Mineral Resources, Open-file Report 141, 162 p.

Eggleston, T.L., Osburn, G.R., and Chapin, C.E., 1983, Third day road log from Socorro to San Antonio, Nogal Canyon, Chupadera Mountains, Luis Lopez manganese district, and the MCA mine: New Mexico Geological Society, Guidebook 34, p. 61–79.

Gardner, J.N., and Goff, F., 1984, Potassium-argon dates from the Jemez volcanic field: Implications for tectonic activity in the north-central Rio Grande rift: New Mexico Geological Society, Guidebook 35, p. 75–81.

Greeley, R., and Iversen, J.D., 1981, Eolian processes and features at Amboy lava field, California: UNESCO Workshop on Physics of Desertification, Proceedings, 23 p.

Gustavson, T.C., 1991, Arid basin depositional systems and paleosols: Fort Hancock and Camp Rice Formations (Pliocene-Pleistocene), Hueco Bolson, west Texas and adjacent Mexico: Texas Bureau of Economic Geology, Report of Investigations 198, 49 p.

Hawley, J.W., Kottlowski, F.E., Strain, W.S., Seager, W.R., King, W.E., and LeMone, D.V., 1969, The Santa Fe Group in the south-central New Mexico border region, *in* Kottlowski, F.E., and Lemone, D.V., eds., Border Stratigraphy Symposium: New Mexico Bureau of Mines and Mineral Resources, Circular 104, p. 52–76.

Ingersoll, R.V., Cavazza, W., Baldridge, W.S., and Shafiqullah, M., 1990, Cenozoic sedimentation and paleotectonics of north-central New Mexico: Implications for initiation and evolution of the Rio Grande rift: Geological Society of America Bulletin, v. 102, p. 1280–1296.

Koning, D.J., 2002 (rev. July 2005), Geologic map of the Española 7.5-minute quadrangle, Rio Arriba and Santa Fe counties, New Mexico: New Mexico Bureau of Geology and Mineral Resources, Open-file Geologic Map OF-GM 54, scale 1:24,000.

Koning, D.J., 2003 (rev. 2005), Geologic map of the Chimayó 7.5-minute quadrangle, Rio Arriba and Santa Fe counties, New Mexico: New Mexico Bureau of Geology and Mineral Resources, Open-file Geologic Map OF-GM-71, scale 1:24,000.

Koning, D.J., and Heizler, M.T., this volume, Stratigraphy and sedimentology of the Santa Fe Group adjoining the Little San Pascual Mountains – implications for footwall exhumation and evolution of the Little San Pascual Mountain fault system: New Mexico Geological Society, Guidebook 72.

Koning, D.J., and Manley, K., 2003 (rev. December 2005), Geologic map of the San Juan Pueblo 7.5-minute quadrangle, Rio Arriba and Santa Fe counties, New Mexico: New Mexico Bureau of Geology and Mineral Resources, Open-file Geologic Map OF-GM-70, scale 1:24,000.

Koning, D.J., and Personius, S.F., 2002, Geologic map of the Bernalillo NW quadrangle, Sandoval County, New Mexico: U.S. Geological Survey, Miscellaneous Field Studies Map 2404, scale 1:24,000.

Koning, D.J., Connell, S.D., Morgan, G.S., Peters, L., and McIntosh, W.C., 2005, Stratigraphy and depositional trends in the Santa Fe Group near Española, north-central New Mexico: tectonic and climatic implications: New Mexico Geological Society, Guidebook 56, p. 237–257.

Koning, D.J., Grauch, V.J.S., Connell, S.D., Ferguson, J., McIntosh, W., Slate, J.L., Wan., E., and Baldridge, W.S., 2013, Structure and tectonic evolution of the eastern Española Basin, Rio Grande rift, north-central New Mexico, *in* Hudson, M., and Grauch, V.J.S., eds., New Perspectives on the Rio Grande rift: From Tectonics to Groundwater: Geological Society of America, Special Paper 494, p. 185–219, doi:10.1130/2013.2494(08).

Koning, D.J., Jochems, A.P., Morgan, G.S., Lueth, V., and Peters, L., 2016a, Stratigraphy, gravel provenance, and age of early Rio Grande deposits exposed 1-2 km northwest of downtown Truth or Consequences, New Mexico: New Mexico Geological Society, Guidebook 67, p. 459–478.

Koning, D.J., Aby, S., Grauch, V.J.S., and Zimmerer, M.J., 2016b, Latest Miocene-earliest Pliocene evolution of the ancestral Rio Grande at the Española-San Luis Basin boundary, northern New Mexico: New Mexico Geology, v. 38, no. 2, p. 24–49.

Koning, D.J., Jochems, A.P., and Heizler, M.T., 2018, Early Pliocene paleovalley incision during early Rio Grande evolution in southern New Mexico: New Mexico Geological Society, Guidebook 69, p. 93–108.

Koning, D.J., Heizler, M., and Jochems, A., 2020, Clues from the Santa Fe Group for Oligocene-Miocene paleogeography of the southeastern Colorado Plateau near Grants, New Mexico: New Mexico Geological Society, Special Publication 14, p. 153–166.

Koning, D.J., Chamberlin, R., and Love, D., this volume, Chupadera Mountains, Second-day Road Log: From Socorro to Box Canyon, Northern Chupadera Mountains, Nogal Canyon, and San Antonio: New Mexico Geological Society, Guidebook 72.

Kottlowski, F.E., 1953, Tertiary-Quaternary sediments of the Rio Grande Valley in southern New Mexico: New Mexico Geological Society, Guidebook 4, p. 144–148.

Love, D.W., Celep, E., McCraw, D.J., and Koning, D., this volume, Summary of the stratigraphy of both foot- and hanging-wall exposures of the Cliff fault, southern embayment of the Albuquerque Basin, Socorro County, New Mexico: New Mexico Geological Society, Guidebook 72.

Lozinsky, R.P., and Tedford, R.H., 1991, Geology and paleontology of the Santa Fe Group, southwestern Albuquerque Basin, Valencia County, New Mexico: New Mexico Bureau of Mines and Mineral Resources, Bulletin 132, 35 p.

Lueth, V.W., Rye, R.O., and Peters, L., 2004, $^{40}Ar/^{39}Ar$ data repository for "Sour Gas" hydrothermal jarosite: Ancient to modern acid-sulfate mineralization in the southern Rio Grande Rift: New Mexico Bureau of Geology and Mineral Resources, Argon Open-file Report OF-AR 22, 41 p.

Mack, G.H., 2004, Middle and late Cenozoic crustal extension, sedimentation, and volcanism in the southern Rio Grande rift, Basin and Range, and southern transition zone of southwestern New Mexico, *in* Mack, G.H., and Giles, K.A., eds., The Geology of New Mexico, A Geologic History: New Mexico Geological Society, Special Publication 11, p. 389–406.

Mack, G.H., Salyards, S.L., and James, W.C., 1993, Magnetostratigraphy of the Plio-Pleistocene Camp Rice and Palomas formations in the Rio Grande rift of southern New Mexico: American Journal of Science, v. 293, p. 49–77.

Mack, G.H., Seager, W.R, and Kieling, J., 1994, Late Oligocene and Miocene faulting and sedimentation, and evolution of the southern Rio Grande rift, New Mexico, USA: Sedimentary Geology, v. 92, p. 79–96.

Mack, G.H., Salyards, S.L., McIntosh, W.C., and Leeder, M.R., 1998, Reversal magnetostratigraphy and radioisotopic geochronology of the Plio-Pleistocene Camp Rice and Palomas formations, southern Rio Grande rift: New Mexico Geological Society, Guidebook 49, p. 229–236.

Mack, G.H., Seager, W.R., Leeder, M.R., Perez-Arlucea, M., and Salyards, S.L., 2006, Pliocene and Quaternary history of the Rio Grande, the axial river of the southern Rio Grande rift, New Mexico, USA: Earth-Science Reviews, v. 79, p. 141–162.

Manley, K., 1976, The late Cenozoic history of the Española Basin, New Mexico [Ph.D. thesis]: Boulder, University of Colorado, 171 p.

Manley, K., 1979, Tertiary and Quaternary stratigraphy of the Northeast Plateau, Española Basin, New Mexico: New Mexico Geological Society, Guidebook 30, p. 231–236.

Minor, S.A., Hudson, M.R., Grauch, V.J.S., and Sawyer, D.A., 2006, Structure of the Santo Domingo Basin and La Bajada constriction area; Chapter E, *in* Minor, S.A., ed., The Cerrillos Uplift, the La Bajada Constriction, and Hydrogeologic Framework of the Santo Domingo Basin, Rio Grande Rift, New Mexico: U.S. Geological Survey, Professional Paper 1720, p. 91–115.

Minor, S.A., Hudson, M.R., Caine, J.S., and Thompson, R.A., 2013, Oblique transfer of extensional strain between basins of the middle Rio Grande rift, New Mexico: Fault kinematic and paleostress constraints, *in* Hudson, M., and Grauch, V.J.S., eds., New Perspectives on the Rio Grande rift: From Tectonics to Groundwater: Geological Society of America, Special Paper 494, p. 345–382, doi:10.1130/2013.2494(14).

Newell, H.H., 1997, $^{40}Ar/^{39}Ar$ geochronology of Miocene silicic lavas in the Socorro–Magdalena area, New Mexico [M.S. thesis]: Socorro, New Mexico Institute of Mining and Technology, 190 p.

NMBGMR [New Mexico Bureau of Geology and Mineral Resources], 2003, Geologic Map of New Mexico, 1:500,000: New Mexico Bureau of Geology and Mineral Resources.

Osburn, G.R., Petty, D.M., and Chapin, C.E., 1981, Geology of the Molina Peak Quadrangle: New Mexico Bureau of Mines and Mineral Resources, Open-file Report 139A, 22 p.

PACES [Pan-American Center for Earth and Environmental Studies], 2021, Gravity dataset for the United States Lower 48 states: data obtained from Raed E. Aldouri (University of Texas at El Paso) on September 14; dataset description at http://cybershare-portal.utep.edu/datasets (accessed September 14, 2021).

Personius, S.F., and Jochems, A.P., compilers, 2016, Fault number 2110, West Joyita fault zone, *in* Quaternary fault and fold database of the United States: U.S. Geological Survey website, https://earthquakes.usgs.gov/hazards/qfaults (accessed 01/28/2022).

Repasch, M., Karlstrom, K., Heizler, M., and Pecha, M., 2017, Birth and evolution of the Rio Grande fluvial system in the past 8 Ma: progressive downward integration and the influence of tectonics, volcanism, and climate: Earth-Science Review, v. 168, p. 113–164.

Sanford, A.R., 1968, Gravity survey in central Socorro County, New Mexico: New Mexico Bureau of Mines and Mineral Resources, Circular 91, 14 p.

Seager, W.R., and Mack, G.H., 2003, Geology of the Caballo Mountains, New Mexico: New Mexico Bureau of Geology and Mineral Resources, Memoir 49, 136 p.

Smith, G.A., 2004, Middle to late Cenozoic development of the Rio Grande rift and adjacent regions in northern New Mexico, *in* Mack, G.H., and Giles, K.A., eds., The Geology of New Mexico, A Geologic History: New Mexico Geological Society, Special Publication 11, p. 331–358.

USGS (United States Geological Survey), 2022, Quaternary fault and fold database of the United States, https://www.usgs.gov/programs/earthquake-hazards/faults (accessed April 22, 2022).

Wells, S.G., Dohrenwend, J.C., McFadden, L.D., Turrin, B.D., and Mahrer, K.D., 1985, Late Cenozoic landscape evolution on lava flow surfaces of the Cima volcanic field, Mojave Desert, California: Geological Society of America Bulletin, v. 96, p. 1518–1529.

Appendices can be found at
https://nmgs.nmt.edu/repository/index.cfml?rid=2022002